Self-consistent-charge density-functional tight-binding method for simulations of complex materials properties

M. Elstner
Universität-GH, Paderborn, Fachbereich Physik, Theoretische Physik, D-33098 Paderborn, Germany and Department of Molecular Biophysics, German Cancer Research Center, D-69120 Heidelberg, Germany

D. Porezag, G. Jungnickel, J. Elsner, M. Haugk, and Th. Frauenheim
Universität-GH, Paderborn, Fachbereich Physik, Theoretische Physik, D-33098 Paderborn, Germany

S. Suhai
Department of Molecular Biophysics, German Cancer Research Center, D-69120 Heidelberg, Germany

G. Seifert
Technische Universität, Institut für Theoretische Physik, Mommsenstrasse 13, D-01062 Dresden, Germany
(Received 9 September 1997; revised manuscript received 19 March 1998)

We outline details about an extension of the tight-binding (TB) approach to improve total energies, forces, and transferability. The method is based on a second-order expansion of the Kohn-Sham total energy in density-functional theory (DFT) with respect to charge density fluctuations. The zeroth order approach is equivalent to a common standard non-self-consistent (TB) scheme, while at second order a transparent, parameter-free, and readily calculable expression for generalized Hamiltonian matrix elements may be derived. These are modified by a self-consistent redistribution of Mulliken charges (SCC). Besides the usual ''band structure'' and short-range repulsive terms the final approximate Kohn-Sham energy additionally includes a Coulomb interaction between charge fluctuations. At large distances this accounts for long-range electrostatic forces between two point charges and approximately includes self-interaction contributions of a given atom if the charges are located at one and the same atom. We apply the new SCC scheme to problems where deficiencies within the non-SCC standard TB approach become obvious. We thus considerably improve transferability. [S0163-1829(98)03532-2]

I. INTRODUCTION

Starting with Slater and Koster's work in 1954, tight-binding (TB) theory since then has addressed an important topic of computational material science, namely, the development of rapid, robust, generally transferable and accurate methods to calculate atomic and electronic structures, energies, and forces of larger molecular and condensed systems.

The standard TB method works by expanding eigenstates of a Hamiltonian in an orthogonalized basis of atomiclike orbitals and representing the exact many-body Hamilton operator with a parametrized Hamiltonian matrix, where the matrix elements are fitted to the band structure of a suitable reference system.

Although the original Slater-Koster scheme[1] was only used to investigate the electronic structure of periodic solids, the tight-binding ideas later on have been generalized to an atomistic total-energy method. While Froyen and Harrison in 1979 proposed an r^{-2} dependence of the matrix elements to investigate problems with varying interatomic distances,[2,3] Chadi at the same time applied the method to semiconductor surface energy minimizations.[4] He proposed to write the total energy as a function of all atomic coordinates,

$$E_{\mathrm{tot}} = E_{bs} + E_{\mathrm{rep}}, \tag{1}$$

where E_{bs} is the sum over the occupied orbital energies derived from the diagonalization of the electronic Hamiltonian and E_{rep} is a short-range repulsive two-particle interaction. The latter includes the ionic repulsion and corrections due to approximations made in the first term. The repulsive interactions versus distance may be determined in a parametrized functional form for reproducing cohesive energy and elastic constant (bulk-modulus) data for crystalline systems.

A common actual TB calculation and its results, hence, clearly depend on the parametrization scheme and the transferability to various scale systems and problems is rather limited. Successful applications include (for a review, see Ref. 5) high accuracy band-structure evaluations,[6] band calculations in semiconductor heterostructures,[7] device simulations for optical properties,[8] simulations of amorphous solids,[9] and predictions of low-energy silicon clusters.[10,11] However, if the accuracy of the scheme is particularly tuned for dealing with a certain structure deficiencies may arise when describing bonding situations that were not covered by the parametrization. Nonorthogonality is a step forward to improve transferability.[11]

In order to completely avoid the difficult parametrization within a multiconfigurational space, more sophisticated, yet efficient, TB schemes have recently been developed. These methods include the TB-LMTO (linear-muffin-tin orbitals) method,[12] the Hartree-Fock-based TB,[13] a successful DFT parametrization of TB,[14] the *ab initio* multicenter TB,[15] and our DF-based (two-center) TB approach.[16] Here, the Hamiltonian matrix elements are explicitly calculated within a non-

orthogonal basis of atomic orbitals. These schemes yield accurate results for a broad range of bonding situations, for which the superposition of overlapping atomlike densities serves as a good approximation for the many-atom structure.

The key idea of these developments is to understand the TB approach as a stationary approximation to density-functional (DF) theory.[17–20] In particular it has been proven that (1) is a valid approximation to the total energy of the many-atom structure. Central features of the common methodology, namely, non-self-consistent treatment of the Kohn-Sham equations and the exploitation of pairwise repulsive interactions are now known to be strongly related to an appropriate ''educated guess'' for the inital charge density of the system. Then the total energy is readily computable and second-order effects arising from a charge redistribution are negligibly small.

Nevertheless, problems naturally arise if a delicate charge balance is required for establishing chemical bonding between different types of atoms. In such cases, an adjustment of the charge distribution via a self-consistent field (SCF) procedure may be necessary. Hence, there is a need to extend the TB formalism in order to improve its transferability without discarding the simplicity, speed, and efficiency, which make it so useful.

Within the framework of standard empirical TB theory, several proposals have been made to generalize the TB energies by explicitly considering interatomic electron-electron interactions.[21–24] Skriver and Rosengaard use an efficient self-consistent Green's-function technique based on the LMTO method within the tight-binding and atomic-sphere approximation.[25] Tsai *et al.*[26] improved the *ab initio* multicenter TB scheme[15] in order to account for charge transfer. By using the Ewald technique, they added and subtracted to each atom a Gaussian charge distribution and solved the Schrödinger equation iteratively, to determine the self-consistent atomic charges. Demkov *et al.*[27] used a different approach to modify this TB scheme by including long-ranged Hartree contributions, which leads to a self-consistent adjustment of site-dependent occupation numbers.

Here, we focus on describing in detail the systematic extension of the tight-binding formalism and of our DFTB scheme[16,18] in order to derive a generalized self-consistent charge (SCC) methodology, which has been discussed recently.[28] This differs from previous approaches since we base the modification of the TB total-energy expression in Sec. II on a second-order expansion of the Kohn-Sham energy functional[29] with respect to density fluctuations. This methodology ensures a proper distribution of the charge and overcomes the requirement of local charge neutrality,[19] especially in multicomponent systems. In maintaining the simple two-center picture of the non-SCC standard DFTB, which we briefly summarize in Sec. III, the new scheme, described in more detail in Sec. IV, can be easily incorporated into any standard TB method. In Sec. V, we demonstrate the improvements considering properties of molecular and solid state systems, where the non-SCC scheme failed, and point out recent successful applications to polar semiconductors surfaces and dislocations.

II. DENSITY-FUNCTIONAL BASIS OF TB THEORY

The total energy of a system of M electrons in the field of N nuclei at positions $\vec{R}$ may be written within DFT as a functional of a charge density $n(\vec{r})$:

$$E=\sum_i^{\text{occ}} \langle\Psi_i|-\frac{\Delta}{2}+V_{\text{ext}}+\frac{1}{2}\int' \frac{n(\vec{r}')}{|\vec{r}-\vec{r}'|}|\Psi_i\rangle+E_{\text{XC}}[n(\vec{r})] + \frac{1}{2}\sum_{\alpha,\beta}^{N}\frac{Z_\alpha Z_\beta}{|\vec{R}_\alpha-\vec{R}_\beta|}, \tag{2}$$

where the first sum is over occupied Kohn-Sham eigenstates Ψ_i, the second term is the exchange-correlation (XC) contribution, and the last term covers the ion-ion core repulsion, E_{ii}. Following Foulkes and Haydock,[20] we now rewrite the total energy in order to transform the leading matrix elements. We first substitute the charge density in Eq. (2) by a superposition of a reference or input density $n_0'=n_0(\vec{r}')$ and a small fluctuation $\delta n'=\delta n(\vec{r}')$, $\int d\vec{r}'$ is expressed by $\int'$:

$$E=\sum_i^{\text{occ}} \langle\Psi_i|-\frac{\Delta}{2}+V_{\text{ext}}+\int' \frac{n_0'}{|\vec{r}-\vec{r}'|}+V_{\text{XC}}[n_0]|\Psi_i\rangle - \frac{1}{2}\int\int' \frac{n_0'(n_0+\delta n)}{|\vec{r}-\vec{r}'|}-\int V_{\text{XC}}[n_0](n_0+\delta n) + \frac{1}{2}\int\int' \frac{\delta n'(n_0+\delta n)}{|\vec{r}-\vec{r}'|}+E_{\text{XC}}[n_0+\delta n]+E_{ii}. \tag{3}$$

The second term in this equation corrects for the double counting of the new Hartree, the third term for the new XC contribution in the leading matrix element, and the fourth term comes from dividing the full Hartree energy in Eq. (2) into a part related to n_0 and to δn.

Finally, we expand E_{XC} at the reference density and obtain the total energy correct to second order in the density fluctuations by a simple transformation. Note that the terms linear in δn cancel each other at any arbitrary input density n_0:

$$E=\sum_i^{\text{occ}} \langle\Psi_i|\hat{H}_0|\Psi_i\rangle-\frac{1}{2}\int\int' \frac{n_0'n_0}{|\vec{r}-\vec{r}'|}+E_{\text{XC}}[n_0] - \int V_{\text{XC}}[n_0]n_0+E_{ii} + \frac{1}{2}\int\int'\left(\frac{1}{|\vec{r}-\vec{r}'|}+\left.\frac{\delta^2 E_{\text{XC}}}{\delta n\ \delta n'}\right|_{n_0}\right)\delta n\ \delta n'. \tag{4}$$

III. ZEROTH-ORDER NON-SCC APPROACH, STANDARD DFTB

The traditional non-SCC TB approach is to neglect the last term in this final equation, with $\hat{H}_0$ as the Hamiltonian operator resulting from an input density n_0. As usual, a frozen-core approximation is applied to reduce the computational efforts by only considering the valence orbitals. The Kohn-Sham equations are then solved non-self-consistently and the second-order correction is neglected. The contributions in Eq. (4) that depend on the input density n_0 only and the core-core repulsion are taken to be a sum of one- and

two-body potentials.[20] The latter, denoted by $E_{\rm rep}$, are strictly pairwise, repulsive, and short ranged. The total energy then reads

$$E_0^{\rm TB}=\sum_i^{\rm occ}\langle\Psi_i|\hat{H}_0|\Psi_i\rangle+E_{\rm rep}. \tag{5}$$

To solve the Kohn-Sham equations, the single-particle wave functions Ψ_i within an LCAO ansatz are expanded into a suitable set of localized atomic orbitals φ_ν,

$$\Psi_i(\vec{r})=\sum_\nu c_{\nu i}\varphi_\nu(\vec{r}-\vec{R}_\alpha). \tag{6}$$

As described earlier,[16] we employ confined atomic orbitals in a Slater-type representation. These are determined by solving a modified Schrödinger equation for a free neutral pseudoatom within SCF-LDA calculations.[30] The effective one-electron potential of the many-atom structure in Ref. 16 is approximated as a sum of spherical Kohn-Sham potentials of neutral pseudoatoms due to their *confined* electron density.

By applying the variational principle to the zeroth-order energy functional (5), we obtain the non-SCF Kohn-Sham equations, which, finally, within the pseudoatomic basis, transform into a set of algebraic equations:

$$\sum_\nu^M c_{\nu i}(H^0_{\mu\nu}-\varepsilon_i S_{\mu\nu})=0,\quad \forall\mu,i, \tag{7}$$

$$H^0_{\mu\nu}=\langle\varphi_\mu|\hat{H}_0|\varphi_\nu\rangle,\quad S_{\mu\nu}=\langle\varphi_\mu|\varphi_\nu\rangle,\quad \forall\mu\epsilon\alpha,\quad \nu\epsilon\beta. \tag{8}$$

Consistent with the construction of the effective one-electron potential we neglect several contributions to the Hamiltonian matrix elements $H_{\mu\nu}$ (Ref. 18) yielding

$$H^0_{\mu\nu}=\begin{cases}\varepsilon_\mu^{\text{neutral free atom}} & \text{if } \mu=\nu\\ \langle\varphi_\mu^\alpha|\hat{T}+V_0^\alpha+V_0^\beta|\varphi_\nu^\beta\rangle & \text{if } \alpha\neq\beta\\ 0 & \text{otherwise.}\end{cases} \tag{9}$$

Since indices α and β indicate the atoms on which the wavefunctions and potentials are centered, only two-center Hamiltonian matrix elements are treated and explicitly evaluated in combination with the two-center overlap matrix elements. As follows from Eq. (9), the eigenvalues of the free atom serve as diagonal elements of the Hamiltonian, thus guaranteeing the correct limit for isolated atoms.

By solving the general eigenvalue problem Eq. (7), the first term in Eq. (5) becomes a simple summation over all occupied Kohn-Sham orbitals ε_i (occupation number n_i), while $E_{\rm rep}$ can easily be determined as a function of distance by taking the difference of the SCF-LDA cohesive and the corresponding TB band-structure energy for a suitable reference system,

$$E_{\rm rep}(R)=\left\{E_{\rm LDA}^{\rm SCF}(R)-\sum_i^{\rm occ} n_i\varepsilon_i(R)\right\}\Bigg|_{\text{reference structure}}. \tag{10}$$

Interatomic forces for molecular-dynamics applications can easily be derived from an explicit calculation of the gradients of the total energy at the considered atom sites,

$$M_\alpha\ddot{\vec{R}}_\alpha=-\frac{\partial E_0^{TB}}{\partial\vec{R}_\alpha}=-\sum_i n_i\sum_\mu\sum_\nu c_{\mu i}c_{\nu i}\left[\frac{\partial H^0_{\mu\nu}}{\partial\vec{R}_\alpha}-\varepsilon_i\frac{\partial S_{\mu\nu}}{\partial\vec{R}_\alpha}\right]-\sum_{\beta\neq\alpha}\frac{\partial E_{\rm rep}(|\vec{R}_\alpha-\vec{R}_\beta|)}{\partial\vec{R}_\alpha}. \tag{11}$$

This is the non-SCC DFTB approach, which has been successfully applied to various problems in different systems and materials, covering carbon,[16] silicon,[31] and germanium structures,[32] boron and carbon nitrides,[33,34] silicon carbide[35] and oxide[36] and GaAs surfaces.[37] Provided an educated guess of the initial or input charge density of the system, the energies and forces are correct to second order of charge density fluctuations. Furthermore, the short-range two-particle repulsion (determined once using a proper reference system) operates transferably in very different bonding situations considering various scale systems.

IV. SECOND-ORDER SELF-CONSISTENT CHARGE EXTENSION, SCC-DFTB

The previous scheme discussed above is suitable when the electron density of the many-atom structure may be represented as a sum of atomiclike densities in good approximation. The uncertainties within the standard DFTB variant, however, increase if the chemical bonding is controlled by a delicate charge balance between different atomic constituents, especially in heteronuclear molecules and in polar semiconductors. Therefore, we have extended the approach in order to improve total energies, forces, and transferability in the presence of considerable long-range Coulomb interactions. We start from Eq. (4) and now explicitly consider the second-order term in the density fluctuations.

In order to include associated effects in a simple and efficient TB concept, we first decompose $\delta n(\vec{r})$ into atom-centered contributions, which decay fast with increasing distance from the corresponding center. The second-order term then reads

$$E_{\rm 2nd}=\frac{1}{2}\sum_{\alpha,\beta}^N\int\int'\Gamma[\vec{r},\vec{r}',n_0]\delta n_\alpha(\vec{r})\,\delta n_\beta(\vec{r}'), \tag{12}$$

where we have used the functional Γ to denote the Hartree and XC coefficients. Second, the δn_α may be expanded in a series of radial and angular functions:

$$\delta n_\alpha(\vec{r})=\sum_{l,m}K_{ml}F^\alpha_{ml}(|\vec{r}-\vec{R}_\alpha|)Y_{lm}\left(\frac{\vec{r}-\vec{R}_\alpha}{|\vec{r}-\vec{R}_\alpha|}\right)\approx\Delta q_\alpha F^\alpha_{00}(|\vec{r}-\vec{R}_\alpha|)Y_{00}, \tag{13}$$

where F^α_{ml} denotes the normalized radial dependence of the density fluctuation on atom α for the corresponding angular momentum. While the angular deformation of the charge density, e.g., in covalently bonded systems, is usually described very well within the non-SCC approach, charge transfers between different atoms are not properly handled in

many cases. Truncating the multipole expansion (5) after the monopole term accounts for the most important contributions of this kind while avoiding a substantial increase in the numerical complexity of the scheme. Also, it should be noted that higher-order interactions decay much more rapidly with increasing interatomic distance. Finally, expression (13) preserves the total charge in the system, i.e., $\Sigma_\alpha \Delta q_\alpha = \int \delta n(\vec{r})$. Substitution of Eq. (13) into Eq. (12) yields the simple final expression for the second-order energy term:

$$E_{2\mathrm{nd}} = \frac{1}{2}\sum_{\alpha,\beta}^{N} \Delta q_\alpha \Delta q_\beta \gamma_{\alpha\beta}, \tag{14}$$

where

$$\gamma_{\alpha\beta} = \int\int' \Gamma[\vec{r},\vec{r}',n_0] \frac{F_{00}^{\alpha}(|\vec{r}-\vec{R}_\alpha|) F_{00}^{\beta}(|\vec{r}'-\vec{R}_\beta|)}{4\pi} \tag{15}$$

is introduced as shorthand. In the limit of large interatomic distances, the XC contribution vanishes within LDA and $E_{2\mathrm{nd}}$ may be viewed as a pure Coulomb interaction between two point charges Δq_α and Δq_β. In the opposite case, where the charges are located at one and the same atom, a rigorous evaluation of $\gamma_{\alpha\alpha}$ would require the knowledge of the actual charge distribution. This could be calculated by expanding the charge density into an appropriate basis set of localized orbitals. In order to avoid the numerical effort associated with a basis set expansion of δn and to consider—at least approximately the self-interaction contributions—we apply a simple approximation for $\gamma_{\alpha\alpha}$, which is widely used in semiempirical quantum chemistry methods relying on Parisers observation[38] that $\gamma_{\alpha\alpha}$ can be approximated by the difference of the atomic ionization potential and the electron affinity. This is related to the chemical hardness η_α,[39] or the Hubbard parameter U_α: $\gamma_{\alpha\alpha} \approx I_\alpha - A_\alpha \approx 2\eta\alpha \approx U_\alpha$. The expression for $\gamma_{\alpha\beta}$ then only depends on the distance between the atoms α and β and on the parameters U_α and U_β. The latter constants can be calculated for any atom type within LDA-DFT as the second derivative of the total energy of a single atom with respect to the occupation number of the highest occupied atomic orbital. These values are therefore neither adjustable nor empirical parameters. Indeed, the necessary corrections for a TB total energy in the presence of charge fluctuations turns out to be a typical Hubbard-type correlation in combination with a long-range interatomic Coulomb interaction. Common functional forms for $\gamma_{\alpha\beta}$ have been presented by Ohno,[40] Klopman,[41] and Mataga-Nishimoto.[42] However, they may cause severe numerical problems when applied to periodic systems since Coulomb-like behavior is only accomplished for large interatomic distances. Using expressions like that in Refs. 40 and 41 for periodic systems yield ill-conditioned energies with respect to the Hubbard parameters, i.e., small changes in the Hubbard parameters may result in considerable variations of the total energy, and can therefore not be used.

In order to obtain a well-defined expression useful for all scale systems and consistent with the previous approximations we make an analytical approach to obtain the functional $\gamma_{\alpha\beta}$. In accordance with the Slater-type orbitals used as a basis set to solve the Kohn-Sham equations,[16] we assume an exponential decay of a normalized spherical charge densities

$$n_\alpha(r) = \frac{\tau_\alpha^3}{8\pi} e^{-\tau_\alpha|\vec{r}-\vec{R}_\alpha|}.$$

Neglecting for the moment the second-order contributions of E_{XC} in Eq. (12) we obtain:

$$\gamma_{\alpha\beta} = \int\int' \frac{1}{|r-r'|} \frac{\tau_\alpha^3}{8\pi} e^{-\tau_\alpha|\vec{r}'-\vec{R}_\alpha|} \frac{\tau_\beta^3}{8\pi} e^{-\tau_\beta|\vec{r}-\vec{R}_\beta|}.$$

Integration over r' gives

$$\gamma_{\alpha\beta} = \int \left[\frac{1}{|\vec{r}-\vec{R}_\alpha|} - \left(\frac{\tau_\alpha}{2} + \frac{1}{|\vec{r}-\vec{R}_\alpha|} \right) e^{-\tau_\alpha|\vec{r}-\vec{R}_\alpha|} \right] \times \frac{\tau_\beta^3}{8\pi} e^{-\tau_\beta|\vec{r}-\vec{R}_\beta|}. \tag{16}$$

Setting $R = |R_\alpha - R_\beta|$, after some coordinate transformations one gets (see Appendix)

$$\gamma_{\alpha\beta} = \frac{1}{R} - S(\tau_\alpha, \tau_\beta, R). \tag{17}$$

S is an exponentially decaying short-range function (see Appendix) with

$$S(\tau_\alpha, \tau_\alpha, R) \overset{R\to 0}{=} \frac{5}{16}\tau_\alpha + \frac{1}{R}. \tag{18}$$

If we assume that at $R = 0$ the second order contribution can be expressed approximately via the so-called chemical hardness for a spin-unpolarized atom or Hubbard parameter U_α, we obtain

$$\tfrac{1}{2}\Delta q_\alpha^2 \gamma_{\alpha\alpha} = \tfrac{1}{2}\Delta q_\alpha^2 U_\alpha$$

and therefore from Eq. (18) for the exponents:

$$\tau_\alpha = \tfrac{16}{5} U_\alpha.$$

This result can be interpreted by noting that elements with a high chemical hardness tend to have localized wave functions. The chemical hardness for a spin-unpolarized atom is the derivative of the highest molecular orbital with respect to its occupation number. We calculate this chemical hardness with a fully self-consistent *ab initio* method and therefore include the influence of the second-order contribution of E_{XC} in $\gamma_{\alpha\beta}$ for small distances where it is important. In the limit of large interatomic distances, $\gamma_{\alpha\beta} \to 1/R$ and thus represents the Coulomb interaction between two point charges Δq_α and Δq_β. This accounts for the fact that at large interatomic distances the exchange-correlation contribution vanishes within the local density approximation. In periodic systems, this long range part can be evaluated using the standard Ewald technique, whereas the short-range part S decays exponentially and can therefore be summed over a small number of unit cells. Hence Eq. (17) is a well-defined expression for extended and periodic systems.

Finally, the DFT total energy (4) is conveniently transformed into a transparent TB form,

$$E_2^{\mathrm{TB}}=\sum_i^{\mathrm{occ}} \langle\Psi_i|\hat{H}_0|\Psi_i\rangle+\frac{1}{2}\sum_{\alpha,\beta}^{N} \gamma_{\alpha\beta}\Delta q_\alpha \Delta q_\beta+E_{\mathrm{rep}}, \tag{19}$$

where $\gamma_{\alpha\beta}=\gamma_{\alpha\beta}(U_\alpha,U_\beta,|\vec{R}_\alpha-\vec{R}_\beta|)$. As discussed earlier, the contribution due to $\hat{H}_0$ depends only on n_0 and is therefore exactly the same as in the previous non-SCC studies.[16] However, since the atomic charges depend on the one-particle wave functions Ψ_i, a self-consistent procedure is required to find the minimum of expression (19).

To solve the Kohn-Sham equations, the single-particle wave functions Ψ_i are expanded into a suitable set of localized atomic orbitals φ_ν, denoting the expansion coefficients by $c_{\nu i}$. In accord with the previous scheme,[16] we employ confined Slater-type atomic orbitals. These are determined by solving a modified Schrödinger equation for a free atom within SCF-LDA calculations. By applying the variational principle to the energy functional (19), we obtain the Kohn-Sham equations, which, within the pseudoatomic basis, transform into a set of algebraic equations. We employ the Mulliken charge analysis for estimating the charge fluctuations $\Delta q_\alpha=q_\alpha-q_\alpha^0$,

$$q_\alpha=\frac{1}{2}\sum_i^{\mathrm{occ}} n_i \sum_{\mu\in\alpha}\sum_\nu^{N} (c_{\mu i}^* c_{\nu i} S_{\mu\nu}+c_{\nu i}^* c_{\mu i} S_{\nu\mu}), \tag{20}$$

and obtain

$$\sum_\nu^{M} c_{\nu i}(H_{\mu\nu}-\varepsilon_i S_{\mu\nu})=0, \quad \forall\mu,i, \tag{21}$$

$$H_{\mu\nu}=\langle\varphi_\mu|\hat{H}_0|\varphi_\nu\rangle+\frac{1}{2}S_{\mu\nu}\sum_\xi^{N} (\gamma_{\alpha\xi}+\gamma_{\beta\xi})\Delta q_\xi$$
$$=H_{\mu\nu}^0+H_{\mu\nu}^1, \quad S_{\mu\nu}=\langle\varphi_\mu|\varphi_\nu\rangle, \quad \forall\mu\epsilon\alpha, \quad \nu\epsilon\beta. \tag{22}$$

Since the overlap matrix elements $S_{\mu\nu}$ generally extend over a few nearest-neighbor distances, they introduce multiparticle interactions. The second-order correction due to charge fluctuations is now represented by the nondiagonal Mulliken charge dependent contribution $H_{\mu\nu}^1$ to the matrix elements $H_{\mu\nu}$.

As in our previous studies,[16] we make use of the two-center approximation Eq. (9). Instead of superposing spherical pseudoatom potentials for constructing the effective one-electron potential, however, we now superpose spherical pseudoatom charge densities and evaluate the effective potential for the resulting charge density, $H_{\mu\nu}^0=\langle\varphi_\mu^\alpha|\hat{T}+V(n_0^\alpha+n_0^\beta)|\varphi_\nu^\beta\rangle$ if $\alpha\neq\beta$. Consistent with Eq. (10), we determine the short-range repulsive pair potential E_{rep} as a function of distance by taking the difference of the SCF-LDA cohesive energy and the corresponding SCC-DFTB electronic energy for a suitable reference structure [first two terms in Eq. (19)]. Since charge transfer effects are now considered explicitly, the transferability of E_{rep} is improved compared to the non-SCC approach. A simple analytic expression for the interatomic forces for use in MD simulations is easily derived by taking the derivative of the final TB energy (19) with respect to the nuclear coordinates,

TABLE I. Hydrogenation reactions (kcal/mol) for small organic molecules in comparison with DFT-LSD calculations and experiment (Ref. 39).

Reaction	SCC-DFTB	LSD	exp
$CH_3CH_3+H_2\rightarrow 2CH_4$	20	18	19
$CH_3NH_2+H_2\rightarrow CH_4+NH_3$	23	24	26
$CH_3OH+H_2\rightarrow CH_4+H_2O$	32	28	30
$NH_2NH_2+H_2\rightarrow 2NH_3$	30	43	48
$HOOH+H_2\rightarrow 2H_2O$	101	80	86
$CH_2CH_2+2H_2\rightarrow 2CH_4$	71	67	57
$CH_2NH+2H_2\rightarrow CH_4+NH_3$	66	67	64
$CH_2O+2H_2\rightarrow CH_4+H_2O$	65	67	59
$NHNH+2H_2\rightarrow 2NH_3$	56	89	68
$C_2H_2+3H_2\rightarrow 2CH_4$	124	131	105
$HCN+3H_2\rightarrow CH_4+NH_3$	88	102	76
$CO+3H_2\rightarrow CH_4+H_2O$	83	93	63
$N_2+3H_2\rightarrow 2NH_3$	37	71	37

$$\vec{F}_\alpha=-\sum_i^{\mathrm{occ}} n_i\sum_{\mu\nu} c_{\mu i}c_{\nu i}\left[\frac{\partial H_{\mu\nu}^0}{\partial\vec{R}_\alpha}-\left(\varepsilon_i-\frac{H_{\mu\nu}^1}{S_{\mu\nu}}\right)\frac{\partial S_{\mu\nu}}{\partial\vec{R}_\alpha}\right]$$
$$-\Delta q_\alpha\sum_\xi^{N}\frac{\partial\gamma_{\alpha\xi}}{\partial\vec{R}_\alpha}\Delta q_\xi-\frac{\partial E_{\mathrm{rep}}}{\partial\vec{R}_\alpha}. \tag{23}$$

V. RESULTS

In order to validate the SCC-DFTB approach we now concentrate on presenting results of first successful applications of the SCC-DFTB scheme to a wide class of systems, which are of interest in chemistry, physics, and biology. In particular, we demonstrate the improvements of the method as compared to conventional DFTB and *ab initio* calculations.

A. Organic molecules

For our first benchmark, we have calculated the reaction energies of 36 processes between small closed shell molecules containing oxygen, nitrogen, carbon, and hydrogen from Ref. 43, some of them shown in Table I. We have found a mean absolute deviation from experiment of 12.5 kcal/mol for the SCC-DFTB, compared to 11.1 kcal/mol for the DFT-LSD calculations.[28] Further, considering the optimized geometries of a 63 organic molecules test set from Ref. 44, the mean absolute deviations from experiment in the bond lengths and bond angles are $\Delta R=0.012$ Å and $\Delta\theta=1.80°$,[46] respectively, compared to $\Delta R=0.017$ Å and $\Delta\theta=2.01°$ by using the semiempirical AM1 method.[44]

The improvement over the non-SCC treatment is impressively demonstrated for systems with a delicate counterbalance between ionic and covalent bonding contributions, as, e.g., in formamide (cf. Table II). The DFTB method overestimates the equalization of single and double bonds in the amide and carboxyl groups. This is exclusively due to too much charge flow (of nearly one electron) from carbon to oxygen, clearly indicating the need for a self-consistent charge redistribution. SCC can considerably improve vibrational frequencies of simple molecules, like, for example,

TABLE II. Optimized geometries for three different methods.

Formamide	DFTB	SCC-DFTB	DFT-LSD (Ref. 39)	Expt. (Ref. 39)
C=O	1.296	1.224	1.223	1.193
C−N	1.296	1.382	1.358	1.376
N−H	1.003	0.996	1.022	1.002
C−H	1.130	1.131	1.122	1.102
OCN	127.0	125.5	124.5	123.8

CO_2, in which a wrong charge transfer crucially affects force constants. As in the formamide molecule a too large charge transfer from carbon to oxygen is obtained, connected with an underestimation of the CO bond strength. The symmetric and antisymmetric stretching modes (Σ_g and Σ_u) in CO_2 change from 1458 and 1849 cm^{-1} in DFTB to 1348 and 2305 cm^{-1} in SCC-DFTB in good agreement with the experimental values, 1333 and 2349 cm^{-1}. Frequencies have further been tested for a series of 33 (O-, N-, C-, and H-) containing molecules from Ref. 45 yielding 6.4% mean absolute deviation of vibrational frequencies from the experiment.[46]

B. Biological systems

The very promising results for the organic molecules described above lead us to believe that the method can be applied to investigate the geometric and electronic structure of large biomolecules. A detailed study of H-bonded DNA base pairs and the structure and energetics of different conformers of small polypeptides will be presented elsewhere.[47] Here, we focus only on some examples, where semiempirical methods are known to meet difficulties. We have simulated the retinal in the bacteriorhodopsin molecule, a polyene structure linked via a Schiff base to the protein matrix. The SCC-DFTB geometries are in good agreement with the experimentally reported crystalline structure of the retinal.[48] In particular, the planar structure of the retinal Schiff base is correctly described, characteristics that classical force field and standard semiempirical methods have been reported to fail.[49,50] Another important property for a realistic simulation of structural and energetic properties of peptides and proteins is the rotational barrier in formamide. This is so largely underestimated by semiempirical methods that it is usual to correct for the associated effects by empirical force fields. In contrast, the SCC-DFTB barrier height is in good agreement with the experiments deviating by only 10%.

Since DFT-LDA is known to perform poorly for H-bonded systems, one has to go beyond this level of description. One natural extension provides the use of gradient-corrected functionals such as the PBE-GGA.[51] By applying this functional in both the full SCF reference calculations and the construction of the TB Hamiltonian (GGA atoms and matrix calculations by superposition of densities),[46] the effects of hydrogen bonding within the SCC-DFTB may be described at a corresponding level of accuracy. For example, for the water dimer the linear structure is found to be the global minimum and the O···O distance is underestimated by 4% with respect to the experimental value, which is comparable to the performance of DFT-GGA methods. In order to test the SCC-DFTB for these systems systematically, we calculated the bonding energies of 18 weak and strong hydrogen bonded compounds and studied barriers for proton transfer in katonic and anionic systems.[46] Although some well-known deficiencies of DFT-GGA calculations (concerning the underestimation of proton barriers) cannot be overcome, the overall description is reliable yielding a clear improvement compared to semi-empirical AM1 and PM3 Hamiltonians.

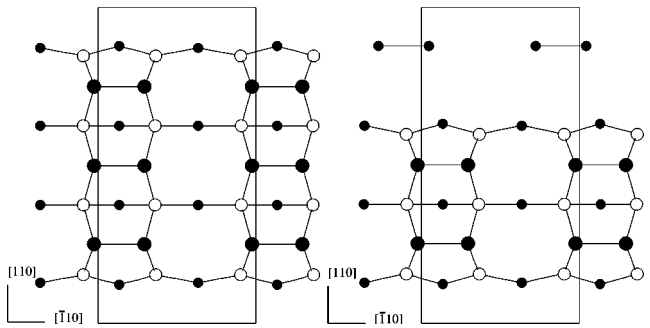

FIG. 1. Top view of the relaxed three As dimers $\beta(2\times4)$ (left) and two As dimers $\beta2(2\times4)$ (right) reconstructions of the GaAs(100) surface. Large (small) filled circles represent top (third) layer As, empty circles Ga atoms. Due to electrostatic effects, the $\beta2(2\times4)$ reconstruction has a lower surface energy.

C. III-V semiconductor surfaces

We then applied the SCC-DFTB method to periodic structures of III-V semiconductors. At first we considered the energetic ordering of reconstructions of GaAs(100) surfaces. The stability of different models that could explain a (2×4) periodicity has been discussed for a long time.[52–56] In particular uncertainty persisted on whether the (2×4) periodicity observed under As-rich growth conditions corresponds to the $\beta(2\times4)$ reconstruction with three surface dimers per (2×4) unit cell or to the $\beta2(2\times4)$ model with two surface dimers (see Fig. 1).

While Ohno found the $\beta(2\times4)$ reconstruction to be energetically favorable, which appeared to be in agreement with an STM observation,[53] Northrup *et al.*[55] and Moll *et al.*[56] determined the $\beta2(2\times4)$ phase to have a lower energy, explaining the high resolution STM images by Hashizume *et al.*[57] Also the SCC-DFTB scheme favors the $\beta2(2\times4)$ model by 3.7 meV/Å^2, which agrees very well with the 3 meV/Å^2 found by Northrup *et al.* who suggested that the calculated energy difference between the $\beta2(2\times4)$ and the $\beta(2\times4)$ phase can be attributed to electrostatic interactions on the surface. As standard TB schemes neglect these interactions it is not surprising that TB calculations by Chadi[52] and calculations with the non-self-consistent DFTB scheme[37] yield degenerate energies for these phases. An analogous question arises in the Ga-rich environment where a three Ga dimer $\beta(4\times2)$ and a two dimer $\beta2(4\times2)$ model could account for the observed (4×2) periodicity. Again the standard DFTB method gives degenerate surface energies, whereas charge self-consistency favors the $\beta2(4\times2)$ reconstruction in agreement with previous scf calculations[55,56] and STM investigations.[58] Figure 2 shows the surface energies determined with the SCC-DFTB method depending on the

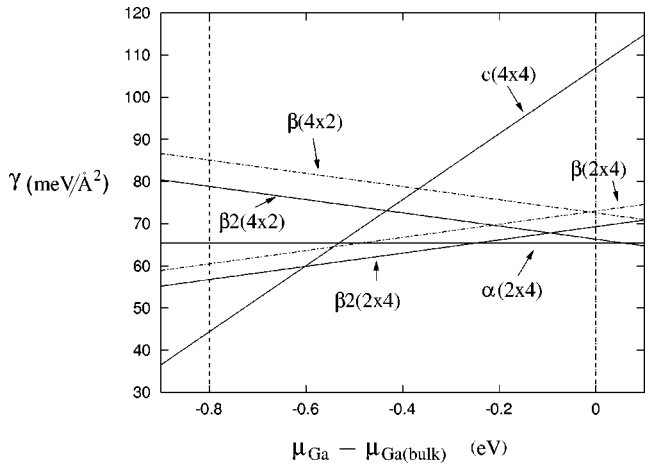

FIG. 2. Surface energies in meV/Å^2 of the GaAs(100) structures plotted versus μ_{Ga}-$\mu_{Ga_{bulk}}$. The part on the right (left) of the diagram corresponds to Ga (As) rich growth conditions.

growth conditions described via the chemical potential μ_{Ga}. They are in very good agreement with the recent SCF-LDA results by Moll *et al.*[56]

Applied to point defects in GaAs SCC-DFTB can be used to describe the energetic ordering for different charge states. Assuming the electrochemical potential μ_e at the valence band edge we obtain for the energy difference between the neutral and the threefold negatively charged Ga vacancy -1.0 eV and for the energy difference between the positively charged As vacancy and the threefold positively charged As vacancy 1.1 eV. In agreement with SCF calculations[59] we can therefore conclude that in *p*-type material the Ga vacancy should exist in its neutral charge state and the As vacancy should be singly positively charged. These conclusions could not be achieved within the standard TB approximation, where the Coulomb repulsion of charge localized at the defect is neglected resulting in significantly lower energies for the charged configurations.

As a final example, we consider the GaN $(10\bar{1}0)$ surface (Fig. 3). The geometry is already well described within the standard DFTB method (cf. Table III) yielding a rehybridization of the surface Ga (N) atoms towards sp^2 (p^3). In this configuration the *N*-derived surface states are occupied whereas the Ga surface states are empty. The surface energy estimated within SCC-DFTB is 121 meV/Å^2, in very good agreement with 118 meV/Å^2 given by Northrup *et al.*[60] We calculated the surface projected SCC-DFTB band structure of the valence bands (see Fig. 4). Again this agrees well with the SCF LDA calculations of Northrup *et al.*[60] However, within the standard TB approximation no correction is applied to the negatively charged *N*-derived surface level. In contrast to a self-consistent treatment the energy of this level is therefore considerably too low, resulting in a surface band shifted at the edges of the Brillouin zone.

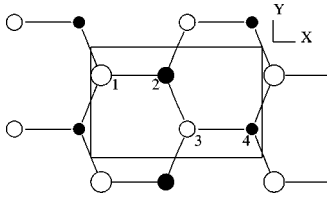

FIG. 3. Schematic top view of the $(10\bar{1}0)$ surface of wurtzite GaN. Atoms 1 and 2 form a dimer in the surface layer. Atoms 3 and 4 form the second layer.

TABLE III. Atomic displacements in Å for the top two layers of atoms at the GaN$(10\bar{1}0)$ surface. Atom numbers refer to Fig. 3. Values in brackets are results of Ref. 50.

Atom	Δx	Δy	Δz
1 ($Ga_{3\times coord.}$)	-0.10 (-0.11)	0.0	-0.23 (-0.20)
2 ($N_{3\times coord.}$)	0.03 (0.01)	0.0	-0.01 (0.02)
3 ($Ga_{4\times coord.}$)	0.01 (0.05)	0.0	0.08 (0.05)
4 ($N_{4\times coord.}$)	0.04 (0.05)	0.0	0.07 (0.05)

As a first successful application of the SCC-DFTB scheme to extended defects we modeled GaN threading screw and edge dislocations in large supercells containing 576 atoms.[61] Consistent with experiments we found that these line defects are electrically inactive, i.e., they do not exhibit deep gap states.

We would like to remark that the time-limiting step in both non-SCC and SCC-DFTB calculations is the solution of the general eigenvalue problem. While the non-SCC scheme requires this task to be solved once for each ionic molecular-dynamics time step, SCC-DFTB needs only a few (3–5) iterations. That means that SCC-DFTB is only slightly less efficient than the non-SCC approach.

VI. SUMMARY

We have presented a straightforward extension and successful implementation of the standard TB theory to operation in a self-consistent charge mode based on a second-order expansion of the Kohn-Sham total-energy functional as calculated within DFT. By this we successfully address a key problem of electronic structure theory, the development of robust, accurate, rapid, and generally transferable methods

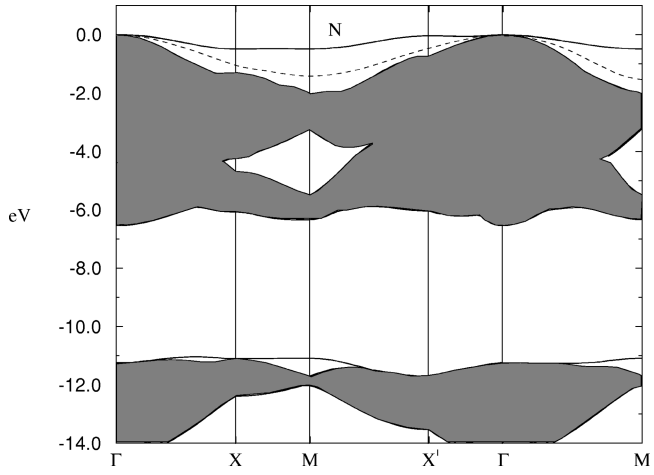

FIG. 4. Valence band structure of the relaxed GaN $(10\bar{1}0)$ surface. The full line represents the *N*-derived surface band calculated with charge self-consistent tight binding (SCC-DFTB), the dashed line the too low-lying surface band determined with non-SCC-DFTB. The shaded region corresponds to the bulk projected band structure.

for *ab initio* based simulation and characterization of large scale molecular and condensed systems. The analytically derived charge-dependent contribution to the total-energy expression can be physically interpreted to describe the chemical hardness for vanishing distances and to represent the Coulomb interaction between point charges at large distances. Moreover, for intermediate distances the energy correction does not contain any empirical functional but is entirely consistent with approximations that frequently enter TB schemes. We show that the scheme is numerically stable for all scale systems and by describing various benchmark-results clearly demonstrate the method's successful operation at sufficient accuracy on very different systems and materials, including up-to-date results for large-scale biomolecules, GaAs surface reconstructions and extended defects in group-III nitrides. This clearly shows the usefulness of the scheme for improving various TB applications in material science.

The method can be understood as a general SCC extension of TB theory offering the great advantage to incorporate any atom type in a straightforward manner. This will not only stimulate MD applications for large-scale semiconductor structures and biological systems, but also for other challanging types of materials.

ACKNOWLEDGMENTS

We thank Th. Köhler, M. Sternberg, and E. Tajkhorshid for helpful discussions, and gratefully acknowledge support from the DFG, DAAD, and US-NSF.

APPENDIX

In Eq. (16) we need to evaluate integrals of the form

$$\int_{IR^3} |\vec{r}-\vec{R}_\alpha|^n e^{-\tau_\alpha|\vec{r}-\vec{R}_\alpha|} e^{-\tau_\beta|\vec{r}-\vec{R}_\beta|} d\vec{r}. \qquad \text{(A1)}$$

Setting $R=|\vec{R}_\alpha-\vec{R}_\beta|$ and transforming to spheroidal coordinates $\xi=|\vec{r}-\vec{R}_\alpha|+|\vec{r}-\vec{R}_\beta|/R$ and $\eta=(|\vec{r}-\vec{R}_\alpha|-|\vec{r}-\vec{R}_\beta|)/R$ we get for Eq. (A1):

$$\frac{\pi}{4}R^3\frac{R^2}{2}\int_1^\infty d\xi\int_{-1}^1 d\eta(\xi+\eta)^{n+1} \times(\xi-\eta)e^{-(\tau_\alpha+\tau_\beta)(R/2)\xi}e^{-(\tau_\alpha-\tau\beta)(R/2)\eta}.$$

Expanding the product $(\xi+\eta)^{n+1}$ into binomials and using the relation $\int_a^b x^l e^{-\alpha x}dx=\Sigma_{i=0}^{l}[l!/(l-i)!\,\alpha^{i+1}]x^{l-1}e^{-\alpha x}|_a^b$ we finally get with $\gamma=(R/2)(\tau_\alpha+\tau_\beta)$ and $\delta=(R/2)(\tau_\alpha-\tau_\beta)$:

$$\frac{\pi}{4}R^3\frac{R^{n+1}}{2}\sum_{i=0}^{n}\binom{n+1}{i}e^{-\gamma}\left[\left(\sum_{m=0}^{i+1}\frac{(i+1)!}{(i+1-m)!\,\gamma^{m+1}}\right)\times\sum_{m=0}^{n+1-i}\frac{(n+1-i)!}{(n+1-i-m)!\,\delta^{m+1}}[(-1)^{n+1-i-m}e^{\delta}-e^{-\delta}]-\left(\sum_{m=0}^{i}\frac{i!}{(i-m)!\,\gamma^{m+1}}\right)\sum_{m=0}^{n+2-i}\frac{(n+2-i)!}{(n+2-i-m)!\,\delta^{m+1}}\times[(-1)^{n+2-i-m}e^{\delta}-e^{-\delta}]\right].$$

From this we obtain for $\gamma_{\alpha\beta}$ in Eq. (16):

$$\frac{1}{R}-\left[e^{-\tau_\alpha R}\left(\frac{\tau_\beta^4\tau_\alpha}{2(\tau_\alpha^2-\tau_\beta^2)^2}-\frac{\tau_\beta^6-3\tau_\beta^4\tau_\alpha^2}{(\tau_\alpha^2-\tau_\beta^2)^3R}\right)+e^{-\tau_\beta R}\left(\frac{\tau_\alpha^4\tau_\beta}{2(\tau_\beta^2-\tau_\alpha^2)^2}-\frac{\tau_\alpha^6-3\tau_\alpha^4\tau_\beta^2}{(\tau_\beta^2-\tau_\alpha^2)^3R}\right)\right].$$

Denoting the function in square brackets with S, we see that S decays exponentially with R. Expanding the exponentials we find the relation (18).

[1] P. C. Slater and G. F. Koster, Phys. Rev. **94**, 1498 (1954).
[2] S. Froyen and W. A. Harrison, Phys. Rev. B **20**, 2420 (1979).
[3] W. A. Harrison, Phys. Rev. B **34**, 2787 (1986).
[4] D. J. Chadi, Phys. Rev. Lett. **43**, 43 (1979).
[5] C. M. Goringe, D. R. Bowler, and E. Hernandez, Rep. Prog. Phys. **60**, 1447 (1997).
[6] J.-M. Jancou, R. Scholz, F. Beltram, and F. Bassani, Phys. Rev. B **57**, 6493 (1998).
[7] R. Scholz, J.-M. Jancou, and F. Bassani, in *Tight-binding Approach to Computational Materials Science,* edited by P. Turchi, A. Gonis, and L. Colombo, MRS Symp. Proc. No. 491 (Materials Research Society, Pittsburgh, 1998), p. 383.
[8] A. Di Carlo, in *Tight-binding Approach to Computational Materials Science* (Ref. 7), p. 389.
[9] C. Z. Wang, K. M. Ho, and C. T. Chan, Phys. Rev. Lett. **70**, 611 (1993).
[10] P. Ordejon, D. Lebedenko, and M. Menon, Phys. Rev. B **50**, 5645 (1994).
[11] M. Menon and K. R. Subbaswamy, Phys. Rev. B **55**, 9231 (1997).
[12] O. K. Andersen and O. Jepsen, Phys. Rev. Lett. **53**, 2571 (1984).
[13] E. Artacho and F. Yndurain, Phys. Rev. B **44**, 6169 (1991).
[14] R. E. Cohen, M. J. Mehl, and D. A. Papaconstantopoulos, Phys. Rev. B **50**, 14 694 (1994).
[15] O. F. Sankey and D. J. Niklewski, Phys. Rev. B **40**, 3979 (1989).
[16] D. Porezag, Th. Frauenheim, Th. Köhler, G. Seifert, and R. Kaschner, Phys. Rev. B **51**, 12 947 (1995).
[17] J. Harris, Phys. Rev. B **31**, 1770 (1985).
[18] G. Seifert, H. Eschrig, and W. Bieger, Z. Phys. Chem. (Leipzig) **267**, 529 (1986).
[19] A. P. Sutton, M. W. Finnis, D. G. Pettifor, and Y. Ohata, J. Phys. C **21**, 35 (1988).
[20] W. Foulkes and R. Haydock, Phys. Rev. B **39**, 12 520 (1989).
[21] F. Bechstedt, D. Reichardt, and R. Enderlein, Phys. Status Solidi B **131**, 643 (1985).
[22] W. A. Harrison, Phys. Rev. B **31**, 2121 (1985).

[23] J. A. Majewski and P. Vogl, Phys. Rev. B **35**, 9666 (1987).
[24] O. L. Alerhand and E. J. Mele, Phys. Rev. B **35**, 5533 (1987).
[25] L. Skriver and N. M. Rosengaard, Phys. Rev. B **43**, 9538 (1991).
[26] M.-H. Tsai, O. F. Sankey, and J. D. Dow, Phys. Rev. B **46**, 10 464 (1992).
[27] A. A. Demkov, J. Ortega, O. F. Sankey, and M. P. Grumbach, Phys. Rev. B **52**, 1618 (1995).
[28] M. Elstner, D. Porezag, G. Jungnickel, Th. Frauenheim, S. Suhai, and G. Seifert, in *Tight-binding Approach to Computational Materials Science* (Ref. 7), p. 131.
[29] W. Kohn and L. J. Sham, Phys. Rev. **140**, A1133 (1965).
[30] H. Eschrig, *The Optimized LCAO Method and Electronic Structure of Extended Systems* (Akademieverlag, Berlin, 1988).
[31] Th. Frauenheim, F. Weich, Th. Köhler, S. Uhlmann, D. Porezag, and G. Seifert, Phys. Rev. B **52**, 11 492 (1995).
[32] P. Sitch, Th. Frauenheim, and R. Jones, J. Phys.: Condens. Matter **8**, 6873 (1996).
[33] J. Widany, F. Weich, Th. Köhler, D. Porezag, and Th. Frauenheim, Diamond Relat. Mater. **5**, 1031 (1996).
[34] F. Weich, J. Widany, and Th. Frauenheim, Phys. Rev. Lett. **78**, 3326 (1997).
[35] R. Gutierrez, Th. Frauenheim, Th. Köhler, and G. Seifert, J. Mater. Chem. **6**, 1657 (1996).
[36] R. Kaschner, Th. Frauenheim, Th. Köhler, and G. Seifert, J. Comp. Aided Mat. Design **4**, 53 (1997).
[37] M. Haugk, J. Elsner, and Th. Frauenheim, J. Phys.: Condens. Matter **9**, 7305 (1997).
[38] R. Pariser, J. Chem. Phys. **24**, 250 (1956).
[39] R. G. Parr and R. G. Pearson, J. Am. Chem. Soc. **105**, 7512 (1983).
[40] K. Ohno, Theor. Chim. Acta **2**, 219 (1964).
[41] G. Klopman, J. Am. Chem. Soc. **86**, 4550 (1964).
[42] N. Mataga and K. Nishimoto, Z. Phys. Chem. (Frankfurt) **13**, 140 (1957).
[43] J. Andzelm and E. Wimmer, J. Chem. Phys. **96**, 1280 (1992).
[44] J. S. Dewar, E. Zoebisch, E. F. Healy, and J. J. P. Stewart, J. Am. Chem. Soc. **107**, 3902 (1985).
[45] J. A. Pople, H. B. Schlegel, R. Krishnan, D. J. Defrees, J. S. Binkley, M. S. Frisch, R. A. Whiteside, R. F. Hout, and W. J. Hehre, Int. J. Quantum Chem., Quantum Chem. Symp. **15**, 269 (1981).
[46] M. Elstner, D. Porezag, G. Jungnickel, Th. Frauenheim, and S. Suhai (unpublished).
[47] M. Elstner, K. Jalkaanen, T. Frauenheim, and S. Suhai (unpublished).
[48] B. Santarsiero, J. Am. Chem. Soc. **112**, 9416 (1990).
[49] E. Tajkhorsid, B. Paizs, and S. Suhai, J. Phys. Chem. B **101**, 8021 (1997).
[50] B. Tavan, K. Schulten, and D. Oesterhelt, Biophys. J. **47**, 415 (1985).
[51] J. P. Perdew, K. Burke, and M. Ernzerhof, Phys. Rev. Lett. **77**, 3865 (1996).
[52] D. J. Chadi, J. Vac. Sci. Technol. A **5**, 834 (1987).
[53] D. K. Biegelsen, R. D. Bringans, J. E. Northrup, and L. E. Swartz, Phys. Rev. B **41**, 5701 (1990).
[54] T. Ohno, Phys. Rev. Lett. **70**, 631 (1993).
[55] J. E. Northrup and S. Froyen, Phys. Rev. B **50**, 2015 (1994).
[56] N. Moll, A. Kley, E. Pehlke, and M. Scheffler, Phys. Rev. B **54**, 8844 (1996).
[57] T. Hashizume, Q. K. Xue, J. Zhou, A. Ichimiya, and T. Sakurai, Phys. Rev. Lett. **73**, 2208 (1994).
[58] Q. Xue, T. Hashizume, J. M. Zhou, T. Sakata, T. Ohno, and T. Sakurai, Phys. Rev. Lett. **74**, 3177 (1995).
[59] S. B. Zhang and J. E. Northrup, Phys. Rev. Lett. **67**, 2339 (1990).
[60] J. E. Northrup and J. Neugebauer, Phys. Rev. B **53**, 10 477 (1996).
[61] J. Elsner, R. Jones, P. Sitch, D. Porezag, M. Elstner, Th. Frauenheim, M. Heggie, S. Öberg, and P. Briddon, Phys. Rev. Lett. **79**, 3672 (1997).